Inorg. Chem. **2006**, *45*, 5767–5773

Structural and Magnetic Properties of $[BDTA]_2[MCl_4]$ [M = Cu (1), Co (2), and Mn (3)], Revealing an $S = {}^1/_2$ Square-Lattice Antiferromagnet with Weak Magnetic Exchange

Sarah S. Staniland,[†,‡] Andrew Harrison,*[,†,‡] Neil Robertson,[†,‡] Konstantin V. Kamenev,[‡,§] and Simon Parsons[†,‡]

The School of Chemistry and EaStChem, The University of Edinburgh, The King's Buildings, Edinburgh EH9 3JJ, U.K., The Centre for Science at Extreme Conditions, Erskine Williamson Building, The King's Buildings, The University of Edinburgh, Edinburgh EH9 3JZ, U.K., and School of Engineering & Electronics, The University of Edinburgh, The King's Buildings, Edinburgh EH9 3JZ, U.K.

Received November 23, 2005

We report the synthesis and structural and magnetic characterization of model square or rectangular antiferromagnets $[BDTA]_2[MCl_4]$ [BDTA = benzo-1,3,2-dithiazolyl; M = Cu (**1**), Co (**2**), and Mn (**3**)]. All of these compounds display a molecular structure of sandwich layers of $[MCl_4]^{2-}$ between two sheets of $[BDTA]^+$ molecules. Consideration of likely superexchange pathways suggests that **1** presents a model square lattice of $S = {}^1/_2$ moments, while **2** and **3** present model rectangular lattices with $S = {}^3/_2$ and ${}^5/_2$, respectively. Magnetic susceptibility measurements indicate that all of these materials have modest antiferromagnetic exchange fields, with near-neighbor exchange J/k_B running from 0.018(1) through 0.35(3) to 2.10(2) K as M runs from Mn to Co to Cu. No signature of any three-dimensional magnetic ordering could be observed down to 1.8 K. **1** is of particular interest because it belongs to a similar class of magnets as the high-T_c superconducting cuprates but has a much smaller exchange field; it has been proposed that the application of a magnetic field to this type of magnet can induce novel quantum states in this class of magnet, but the observation of such states is only experimentally feasible for small exchange. More detailed characterization of **1** by heat capacity measurements showed a broad cusp centered at 1.3 K in the absence of an applied magnetic field but failed to observe any sign of long-range order down to 0.33 K; this suggests that interplane magnetic exchange is weak.

Introduction

Transition-metal halides provide a rich source of low-dimensional magnets owing to their structural diversity and the variety of M−X−M and M−X−X−M bridges that may provide superexchange pathways of varying strength and sign, where M is the metal ion and X the halide.[1−3] It is still difficult to predict the type of structure that a particular new compound will chose, but there are a number of directing influences that may be employed to favor a specific, desired structure type in producing new model magnets.[4] So, if a layered or chainlike material is required, the presence of relatively large, flat molecules with delocalized π electrons may provide either a stacked or a layered motif for the structure,[5] around which chainlike or layered structures of halometalate species may form,[6] yielding pseudo-one- or two-dimensional (1D or 2D) magnetic materials, respectively.

We report the structures and magnetic properties of three new MCl_4^{2-} salts [M = Cu (**1**), Co (**2**), and Mn (**3**)] containing the planar, conjugated, sulfur-rich, and delocalized phenyl and N,S-heterocyclic fused cation $[BDTA]^+$ (BDTA

* To whom correspondence should be addressed. E-mail: a.harrison@ed.ac.uk.
† The School of Chemistry and EaStChem.
‡ The Centre for Science at Extreme Conditions.
§ School of Engineering & Electronics.

(1) Collins, M. F.; Petrenko, O. A. *Can. J. Phys.* **1997**, *75*, 605.
(2) Mitzi, D. B. *Prog. Inorg. Chem.* **1999**, *48*, 1.
(3) de Jongh, L. J.; Miedema, A. R. *Adv. Phys.* **2001**, *50*, 947.
(4) Harrison, A. *J. Phys.: Condens. Matter* **2004**, *16*, S553.
(5) Uji, S.; Shinagawa, H.; Terashima, T.; Yakabe, T.; Terai, Y.; Tokumoto, M.; Kobayashi, A.; Tanaka, H.; Kobayashi, H. *Nature* **2001**, *410*, 908.
(6) Halvorson, K. E.; Patterson, C.; Willett, R. D. *Acta Crystallogr., Sect. B: Struct. Sci.* **1990**, *B46*, 508.

10.1021/ic052024i CCC: $33.50
Published on Web 06/30/2006

= benzo-1,3,2-dithiazolyl), which has the capacity to form strong intermolecular $\pi-\pi$ interactions. These materials form a layered structure with MCl_4^{2-} anions, forming a 2D square (**1**) and rectangular (**2** and **3**) lattice that are well segregated from one another by two layers of countercations. Among 2D square lattices, it is the $S = {}^1/_2$ case, i.e., that of the Cu^{2+} salt, that is currently of greatest interest because of its relationship to the magnetic, and perhaps also the conducting, behavior of cuprate high-temperature superconductors.[7,8] In the first stages of unravelling of the behavior of such materials, it was proposed[9] that a combination of low-spin, relatively low coordination and Heisenberg spin symmetry enhanced quantum fluctuations in the system and led to nonclassical magnetic ground states and excitations; instead of freezing into an ordered, bipartite Néel array of moments upon cooling, it was suggested that the ground state might be a superposition of states composed of combinations of antisymmetrized spin singlets on pairs of adjacent spin centers. The was called the resonating valence bond model by analogy with Pauling's model for chemical bonding.[10] It is now believed that the 2D $S = {}^1/_2$ (quantum) Heisenberg antiferromagnet on a square lattice (2D QHASL) mainly behaves classically (i.e., possesses a Néel ground state whose low-energy spectrum may be described well by spin waves) with a small degree of renormalization due to quantum fluctuations. However, quantum effects may be made more significant in such materials to the extent that they dominate the collective properties. One way of doing this is to apply a strong magnetic field approaching the saturating value, H_s, at which the moments are all pulled into a parallel alignment. For a square antiferromagnet with the magnetic Hamiltonian

$$H = J \sum_{\langle i,j \rangle} S_i \cdot S_j \qquad (1)$$

the value of H_s is $8JS/g\mu_B$.[11] For the $S = {}^1/_2$ case, the application of a critical field $H^* \cong 0.76H_s$ may induce mixing of the one-magnon excitations and the two-magnon continuum, destabilizing the former[12,13] and producing a new form of the quantum disordered state. However, consideration of the magnitude of the field required to achieve such a state reveals a problem for most model 2D QHASLs. For the layered cuprates and related systems such as $Sr_2CuCl_2O_2$, the magnetic coupling is very large ($J/k_B \cong 1500$ K), corresponding to $H_s \cong 4500$ T.[14] The strong magnetic exchange in such materials also makes it difficult to access the full range of magnetic excitations by neutron scattering, which typically probes processes whose energy is up to about 1000 cm^{-1}. Therefore, a 2D square-lattice material with *weak* magnetic coupling is advantageous for this type of investigation because the energy scale is more accessible experimentally.

Molecular systems such as **1**−**3** have much lower magnetic coupling than cuprate oxides because the magnetic centers are further apart and exchange pathways are provided by a series of covalent bonds and less strong nonbonded interactions. Molecular systems that may model 2D QHASLs with smaller values of J have already been identified and studied: copper formate tetrahydrate and its deuterated relative have $J \cong 72$ K, and aspects of their magnetic behavior are influenced by quantum fluctuations.[15−18] However, they also require impractical fields to probe the behavior above H^* ($H^* > 150$ T). More recently, Cu salts of formula $(5CAP)_2CuX_2$ and $(5CAP)_2CuX_2$ have been produced (where 5CAP is 2-amino-5-chloropyridinium, 5MAP is 2-amino-5-methylpyridinium, and X = Cl and Br),[19−22] and they have significantly weaker exchange, with values of J/k_B, in the range of 1−10 K ($H_{sat} > 3-30$ T). However, they suffer from the disadvantage that they are not very anisotropic magnetically, with the ratio of inter- to intraplane exchange, J'/J, on the order of 0.1; they are also difficult to make in the perdeuterated form necessary for the most incisive neutron scattering measurements.

We report here the synthesis and structural and magnetic characterization of the three new materials **1**−**3** and, further, more detailed magnetic and heat capacity measurements of the Cu compound (**1**) to determine its potential as a good model material for probing field-induced quantum fluctuations in this class of magnet. It has a synthetic advantage over the previous "best" material in this class $(5CAP)_2CuCl_2$ (CAPCC) in that [BDTA]Cl can be synthesized more easily than CAP so custom synthesis of the perdeuterated form for neutron experiments is much less challenging. Our measurements indicate that the ratio J'/J is also likely to be smaller in **1** than in CAPCC.[21,22]

Experimental Section

Synthesis. All metal chlorides used in the synthesis were bought as hydrates from Sigma-Aldrich (99.0% purity) and used as supplied. The starting material [BDTA]Cl was synthesized using methods reported in the literature.[23]

(7) Manousakis, E. *Rev. Mod. Phys.* **1991**, *63*, 1.
(8) Fisher, R. A.; Gordon, J. E.; Phillips, N. E. *Annu. Rev. Phys. Chem.* **1996**, *47*, 283.
(9) Anderson, P. W. *Science* **1987**, *235*, 1196.
(10) Pauling, L. *The Nature of the Chemical Bond*, 3rd ed.; Cornell University Press: Ithaca, NY, 1960.
(11) Bonner, J. C.; Fisher, M. E. *Phys. Rev.* **1964**, *135*, A640.
(12) Osano, K.; Shiba, H.; Endoh, Y. *Prog. Theor. Phys.* **1982**, *67*, 995.
(13) Zhitomirsky, M. E.; Chernyshev, A. L. *Phys. Rev. Lett.* **1999**, *82*, 4536.
(14) Greven, M.; Birgeneau, R. J.; Endoh, Y.; Kastner, M. A.; Matsuda, M.; Shirane, G. *Z. Phys. B: Condens. Matter* **1995**, *96*, 465.
(15) Clarke, S. J.; Harrison, A.; Mason, T. E.; McIntyre, G. J.; Visser, D. *J. Phys.: Condens. Matter* **1992**, *4*, L71.
(16) Ronnow, H. M.; McMorrow, D. F.; Harrison, A. *Phys. Rev. Lett.* **1999**, *82*, 3152.
(17) Ronnow, H. M.; McMorrow, D. F.; Harrison, A.; Youngson, I. D.; Coldea, R.; Perring, T. G.; Aeppli, G.; Syljuasen, O. *J. Magn. Magn. Mater.* **2001**, *236*, 4.
(18) Ronnow, H. M.; McMorrow, D. F.; Coldea, R.; Harrison, A.; Youngson, I. D.; Perring, T. G.; Aeppli, G.; Syljuasen, O.; Lefmann, K.; Rischel, C. *Phys. Rev. Lett.* **2001**, *87*, art. no. 037202.
(19) Hammar, P. R.; Dender, D. C.; Reich, D. H.; Albrecht, A. S.; Landee, C. P. *J. Appl. Phys.* **1997**, *81*, 4615.
(20) Matsumoto, T.; Miyazaki, Y.; Albrecht, A. S.; Landee, C. P.; Turnbull, M. M.; Sorai, M. *J. Phys. Chem. B* **2000**, *104*, 9993.
(21) Woodward, F. M.; Albrecht, A. S.; Wynn, C. M.; Landee, C. P.; Turnbull, M. M. *Phys. Rev. B* **2002**, *65*, art. no. 144412.
(22) Coomer, F. C.; Bondah-Jagalu, V.; Grant, K. J.; Harrison, A.; McIntyre, G. J.; Ronnow, H. M.; Feyerhem, R.; Wand, T.; Meissner, M.; Visser, D.; McMorrow, D. F. *Phys. Rev. B* **2006**, submitted for publication.
(23) Wolmershaeuser, G.; Schnauber, M.; Wilhelm, T. *J. Chem. Soc., Chem. Commun.* **1984**, 573.

All single crystals and microcrystalline samples of [BDTA]$_2$[MCl$_4$] salts were prepared by layering [BDTA]Cl (2 equiv) in EtOH on top of $MCl_2 \cdot 2H_2O$ (1 equiv) dissolved in EtOH and HCl (2 equiv, 10 M). The microcrystalline bulk sample was washed with water, EtOH, and then ether and analyzed by CHN. Anal. Calcd for $C_{12}H_8Cl_4CuN_2S_4$ (**1**): C, 28.05; H, 1.57; N, 5.45. Found: C, 27.94; H, 1.55; N, 5.22. Anal. Calcd for $C_{12}H_8Cl_4CoN_2S_4$ (**2**): C, 28.05; H, 1.57; N, 5.45. Found: C, 27.61; H, 1.29; N, 3.90. Anal. Calcd for $C_{12}H_8Cl_4MnN_2S_4$ (**3**): C, 28.05; H, 1.57; N, 5.45. Found: C, 28.18; H, 1.58; N, 5.55. Powder X-ray diffraction was used to establish that the microcrystalline bulk samples had the same structure as that of the single crystals. The microcrystalline powder sample was then used for magnetic measurements.

X-ray crystallography data of 1: $C_{12}H_8Cl_4CuN_2S_4$, M = 513.83, tetragonal, a = 8.2295(3) Å, c = 25.681(2) Å, U = 1739.26(16) Å^3, T = 150 K, space group $P4_32_12$, Z = 4, μ(Mo Kα) = 2.346 mm^{-1}, 31 544 reflections were measured to θ_{max} = 28.8°, of which 2212 were unique (R_{int} = 0.0362). The final conventional R1 factor [based on F and 1767 data with $F > 4\sigma(F)$] was 0.0270, and wR2 (based on F^2 and all 2212 data) was 0.0734. The final difference map max and min were +0.66 and −0.91 e Å^{-3}, respectively.

X-ray crystallography data of 2: $C_{12}H_8Cl_4CoN_2S_4$, M = 509.17, monoclinic, a = 28.0151(8) Å, b = 8.4963(2) Å, c = 16.3222(5) Å, β = 109.9240(10)°, U = 3652.55(18) Å^3, T = 150 K, space group $C2/c$, Z = 8, μ(Mo Kα) = 1.978 mm^{-1}, 13 038 reflections collected to θ_{max} = 28.8°, of which 4377 were unique (R_{int} = 0.0389) which were used in all calculations. The final conventional R1 factor (3566 data) was 0.0505, and wR2 was 0.1021. The final difference map max and min were +0.52 and −0.39 e Å^{-3}, respectively.

X-ray crystallography data of 3: $C_{12}H_8Cl_4MnN_2S_4$, M = 505.18, monoclinic, a = 28.1046(9) Å, b = 8.5467(2) Å, c = 16.4017(5) Å, β = 109.973(2)°, U = 3702.75(19) Å^3, T = 150 K, space group $C2/c$, Z = 8, μ(Mo Kα) = 1.738 mm^{-1}, 13 108 reflections collected to θ_{max} = 28.9°, of which 4510 were unique (R_{int} = 0.0373), which were used in all calculations. The final conventional R1 factor (3822 data) was 0.0405, and wR2 was 0.089 61. The final difference map max and min were +0.52 and −0.49 e Å^{-3}, respectively.

All X-ray diffraction intensities were collected with Mo Kα radiation on a Bruker SMART APEX CCD diffractometer equipped with an Oxford Cryosystems low-temperature device operating at 150 K. Absorption corrections were applied with the multiscan procedure *SADABS*.[24] The structures were solved by Patterson methods (DIRDIF)[25] and refined by full-matrix least squares against F^2 using all data (CRYSTALS for **1** and *SHELXL-97* for **2** and **3**[26,27]). **2** and **3** are isostructural. H atoms were placed in calculated positions and allowed to ride on their parent atoms. All non-H atoms were modeled with anisotropic displacement parameters.

Magnetic Susceptibility. Measurements of the magnetic susceptibility, χ, were performed on microcrystalline samples of **1**−**3** held in gelatine capsules from 300 to 2 K using a Quantum Design MPMS$_2$ SQUID magnetometer. It was confirmed that, at a temperature T = 2 K, the magnetization increased linearly with applied magnetic fields in the range 0 T ≤ B ≤ 5 T. The magnetic field used in subsequent measurements was 0.01 T.

Heat Capacity. Measurement of the heat capacity, C_p, was conducted on a pressed pellet of powder of **1** with a mass of 8.2 mg and a diameter of 2.5 mm using a Quantum Design PPMS instrument over the temperature range 0.33−200 K. The sample was first cooled in zero field, and then the measurement was conducted as it was warmed. Every data point was fitted with two models. One of them is the so-called "simple" model, which assumes a perfect thermal contact between the sample and the sample platform and, therefore, has only one decay constant for the heat flow.[28] The other one is the so-called "2τ" model, for which it is assumed that the thermal contact between the sample and the sample platform is not perfect and has, therefore, two decay constants.[29] Using a nonlinear, least-squares fitting algorithm, the system compares the solutions to the simple and the 2τ models to the actual measurement, and the values of the parameter that give the smallest fit deviation determine the heat capacity.[30] In all cases, we found the 2τ fitting method to give significantly better results, so the results of this form of analysis were used throughout.

Results and Discussion

Preparation and X-ray Structure. Single crystals of **1**−**3** were prepared by slow diffusion of [BDTA]Cl in EtOH with $CuCl_2 \cdot 2H_2O$ (**1**), $CoCl_2 \cdot H_2O$ (**2**), or $MnCl_2 \cdot H_2O$ (**3**) in HCl and EtOH solutions. Small, yellow/orange (**1**), blue/green (**2**), or pale-peach (**3**) plate-shaped crystals were collected after 3, 10, and 8 days, respectively.

All three structures are composed of discrete anionic and cationic units. It can also be seen that all of the structures are similar; indeed, **2** and **3** are isomorphs and crystallize in the space group $C2/c$, while **1** crystallizes in the higher-symmetry space group $P4_32_12$. These two types of structures are displayed in Figures 1 and 2, which also display selected interatomic distances to which we refer below in the discussion of the magnetic lattices. Within the molecules, the most significant bond lengths are those for S−N within BDTA because these can reliably indicate the charge on this molecule. The S−N bond typically shortens in the cation because of depopulation of the antibonding singly occupied molecular orbital of the neutral molecule. Neutral BDTA has a S−N bond distance of 1.646 Å, whereas [BDTA]Cl·SO_2 has a S−N distance of 1.598 Å.[31] For **1**−**3**, all of the S−N distances are in the range of 1.596−1.604 Å, confirming the cationic character of this component and, hence, the dianionic character of the metal complexes.

All of the structures display a layered motif of two planes of [BDTA]$^+$ ions with [MCl$_4$]$^{2-}$ units sandwiched between them; these sandwich layers then stack on top of each other. In **1**, the [BDTA]$^+$ ions in any particular layer are all oriented in the same direction, but this direction changes between layers: there is a 90° twist to the orientation of the [BDTA]$^+$ ions between a pair of layers in a sandwich, and there is a further 180° twist in moving to the nearest layer in the next

(24) Sheldrick, G. M. *SADABS*; University of Göttingen: Göttingen, Germany, 1997.
(25) Beurskens, P. T.; Beurskens, G.; Bosman, W. P.; de Gelder, R.; Garcia-Granda, S.; Gould, R. O.; Israel, R.; Smits, J. M. M., Crystallography Laboratory, University of Nijmegen, Nijmegen, The Netherlands, 1996.
(26) Sheldrick, G. M. *SHELXL-97*; University of Göttingen: Göttingen, Germany, 1997.
(27) Betteridge, P. W.; Carruthers, J. R.; Cooper, R. I.; Prout, K.; Watkin, D. J. *J. Appl. Crystallogr.* **2003**, *36*, 1487.
(28) Stewart, G. R. *Rev. Sci. Instrum.* **1983**, *54*, 1.
(29) Hwan, J. S.; Lin, K. J.; Tien, C. *Rev. Sci. Instrum.* **1997**, *68*, 94.
(30) *Physical Property Measurement System: Heat Capacity User's Manual*, Quantum Design: San Diego, CA, 2002.
(31) Umezono, Y.; Fujita, W.; Awaga, K. *Chem. Phys. Lett.* **2005**, *409*, 139.

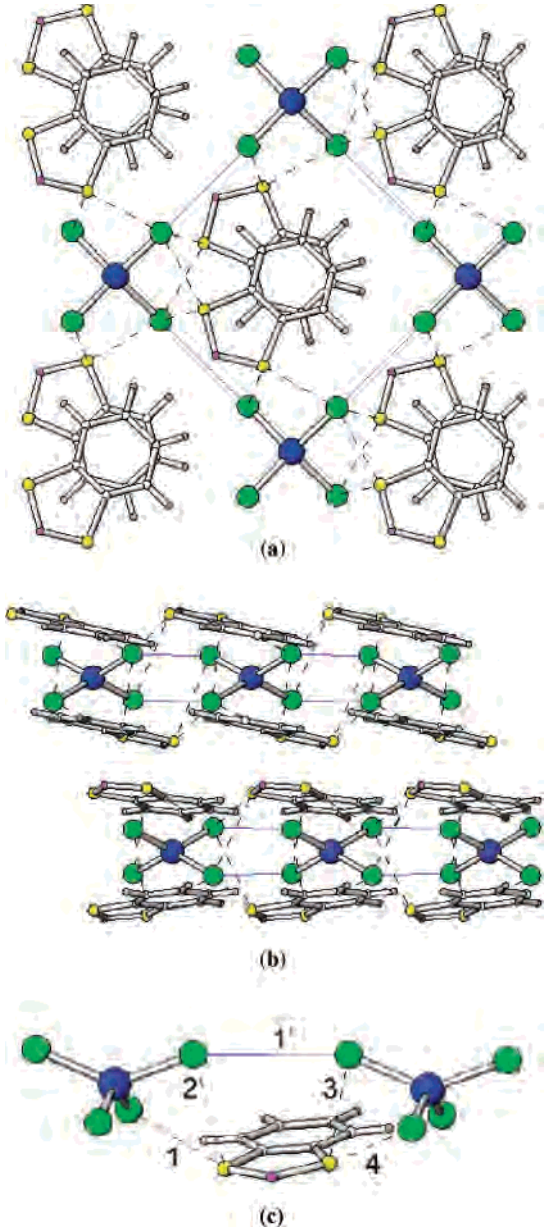

Figure 1. Crystal structure of **1** viewed (a) along the *c* axis, (b) perpendicular to the *c* axis, and (c) in greater detail viewed perpendicular to the [0, 1, 1] plane to pick out the most likely exchange pathways. The dashed lines indicate intermolecular contacts shorter than the sum of the van der Waals radii indicated, and the solid blue lines indicate the shortest Cl−Cl between adjacent $CuCl_4^{2+}$ units. Values for labeled interatomic separations are given in Table 1.

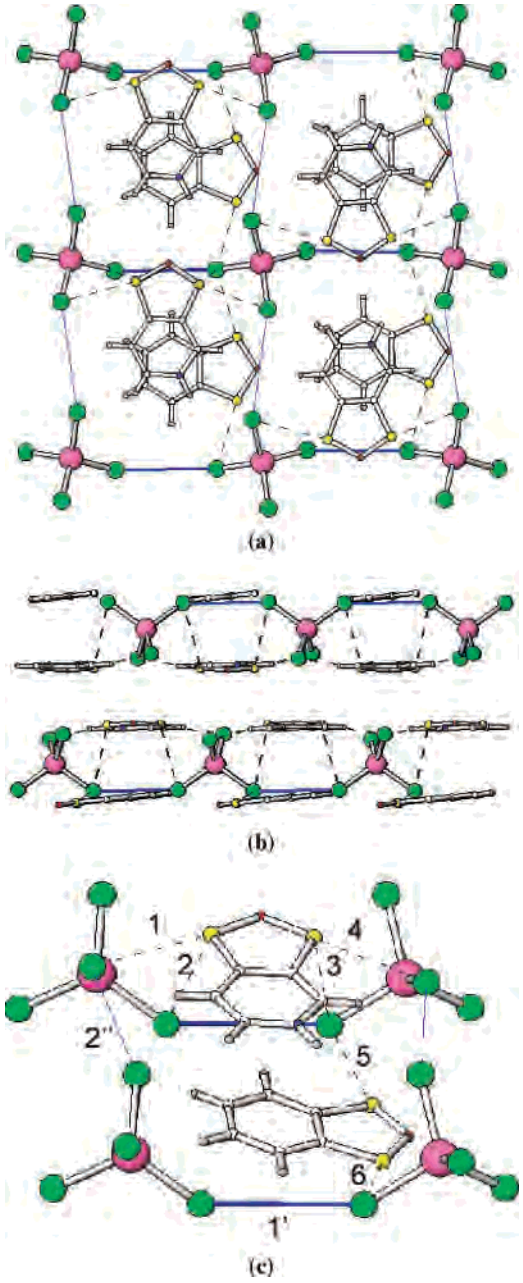

Figure 2. Crystal structure of **3** viewed (a) along the *c* axis, (b) perpendicular to the *c* axis, and (c) in greater detail to pick out the most likely exchange pathways. The dashed lines indicate intermolecular contacts shorter than the sum of the van der Waals radii indicated, and the solid blue lines indicate the shortest Cl−Cl between adjacent $CuCl_4^{2+}$ units. Values for labeled interatomic separations are given in Table 1.

sandwich, giving a repeat unit of four $[BDTA]^+$ ions in the unit cell. **2** and **3** also have a repeat unit of four $[BDTA]^+$ layers in the unit cell, again with an approximately 90° twist to the orientation of the $[BDTA]^+$ ions between a pair of layers in each sandwich; however, within one of the layers of each sandwich, the $[BDTA]^+$ molecules all lie in the same direction, and in the other, they adopt alternate orientations at 180° to each other, leading to an overall centrosymmetric unit cell. The two different structure types also have different arrangements of the $[MCl_4]^{2-}$ units: in **1**, the Cu centers are arranged on a perfectly square grid, 8.229 Å apart, while the array of metal ions in **2** and **3** is rectangular, with centers 8.162 and 8.496 Å apart in **2** and 8.203 and 8.547 Å apart in **3**. In **1**, the $[BDTA]^+$ cation is tilted out of the plane of the sandwich layers by 10.96° and the $[CuCl_4]^{2-}$ anion is distorted toward a square-planar geometry to accommodate this highly symmetrical structure.[32] This type of distortion is most likely for **1**, which is prone to a Jahn−Teller effect, while in **2** and **3**, the $[MCl_4]^{2-}$ anions are not and are therefore likely to deviate little from a tetrahedral conformation, compromising the symmetry of the overall structure.

A key issue in all of these materials is the nature of any lattice of coupled magnetic ions, so we need to consider what

(32) White, D. J.; Cronin, L.; Parsons, S.; Robertson, N.; Tasker, P. A.; Bisson, A. P. *Chem. Commun.* **1999**, 1107.

Table 1. Selected Bond Lengths (Å) That May Be Relevant to Magnetic Exchange Processes in **1**−**3**[a]

	1	2	3
M−M (1)	7.6257	8.1624	8.2027
M−M (2)		8.4963	8.5467
M−M (3)	8.2294	7.6383	7.6435
Cl−S (1)	3.1672	3.3216	3.4129
Cl−S (2)	3.4725	3.3872	3.3683
Cl−S (3)	3.3839	3.4002	3.4459
Cl−S (4)	3.1863	3.2058	3.2173
Cl−S (5)		3.0831	3.1009
Cl−S (6)		3.0782	3.0998
Cl−Cl (1)	4.067	4.4555	4.3568
Cl−Cl (2)		4.8898	4.8104

[a] The numbering of the various Cl−S and Cl−Cl distances is given in Figures 1 and 2. For M−M distances, (1) is the shortest intraplane separation, (2) is the next shortest for **2** and **3**, and (3) is the closest interplane separation.

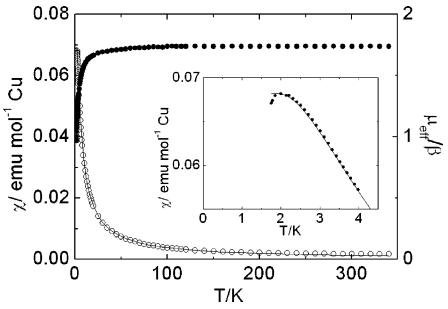

Figure 3. Magnetic susceptibility of **1** as a function of the temperature, with the low-temperature behavior shown in greater detail as an inset. The line through the data represents the best fit of a HTE expression for the susceptibility.

are the most likely pathways for magnetic exchange between metal centers. At first sight, the layered structure of all of the materials and the disposition of the $[MCl_4]^{2-}$ units suggest that **1** presents a square lattice of moments on Cu^{2+}, while **2** and **3** present rectangular lattices of Co^{2+} and Mn^{2+}, respectively. One promising pathway for magnetic exchange involves Cl on the $[MCl_4]^{2-}$ units interacting with S on the delocalized π-electron system on BDTA. In **1**, Cl−S separations for this type of interaction go down to 3.167 Å (though it should be noted that the distance between Cl and S on $[BDTA]^+$ in an *adjacent* sandwich can be as little as 3.613 Å). Likewise, in **2** and **3**, Cl−S separations within the sandwich layers can be less than 3.10 Å (but, again, the distance between Cl and S on $[BDTA]^+$ in an *adjacent* sandwich can be as little as 3.556 Å for **2** and 3.549 Å for **3**). An alternative pathway for superexchange, and one that has been proposed as significant for the 2D QHASL $(5CAP)_2CuCl_2$,[19] is via Cl···Cl contacts: in that case, in-plane and out-of-plane separations were found to be 4.34 and 4.94 Å, respectively, and the corresponding exchange interactions have been estimated as $J/k_B = 1.25$ K and $J'/k_B = 0.3$ K, respectively;[19] in the present case, we find the closest in-plane and out-of-plane Cl···Cl separations in **1** to be 4.067 and >6.3 Å, so the former could be significant in this material, while the latter are likely to be insignificant.

Thus, we anticipate the collective magnetic properties of these materials to be characteristic of square or rectangular arrays with weaker coupling between these layers.

Magnetic Susceptibility. The magnetic susceptibility of **1**−**3**, corrected for the diamagnetism of the gelatin capsule

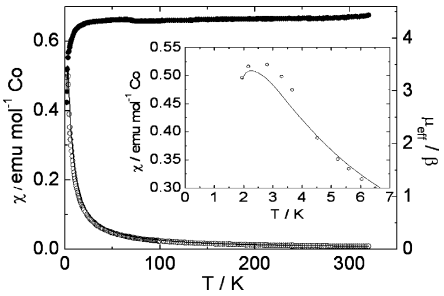

Figure 4. Magnetic susceptibility of **2** as a function of the temperature, with the low-temperature behavior shown in greater detail as an inset. The line through the data represents the best fit of a HTE expression for the susceptibility.

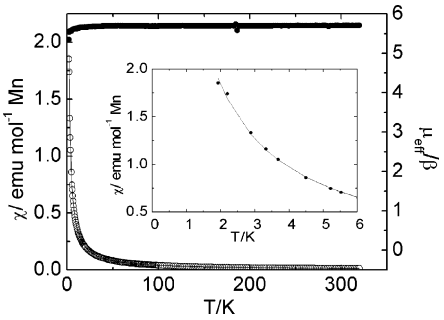

Figure 5. Magnetic susceptibility of **3** as a function of the temperature, with the low-temperature behavior shown in greater detail as an inset. The line through the data represents the best fit of a HTE expression for the susceptibility.

Table 2. Magnetic Parameters for **1**−**3** Extracted from Magnetic Susceptibility Data through Either a Curie−Weiss Fit to the Data or HTE Analysis[a]

compd	C_{so}/ emu K mol^{-1}	C/ emu K mol^{-1}	θ/K	g (HTE)	Jk_B^{-1}/K (HTE)
1	0.375	0.4053(2)	−2.46(1)	2.042(5)	2.10(2)
2	1.875	2.357(2)	−1.57(7)	2.328(5)	0.35(2)
3	4.377	4.041(2)	−0.196(3)	1.931(3)	0.018(1)

[a] C is the Curie parameter and θ the Curie temperature. The table also gives the spin-only (so) value expected for C for each ion.

and the constituent atoms and molecules using Pascal's constants, is shown in Figures 3−5, respectively. Compounds **1** and **2** display a cusp in χ at 2.0 and 2−2.5 K, respectively, indicative of a buildup of antiferromagnetic correlations in the magnetic layers; no such cusp can be seen in the Mn analogue, **3**, suggesting that any such correlations are weaker. At temperatures above 2 or 3 times that of any cusp, the data can be modeled successfully by the Curie−Weiss law, yielding the parameters reported in Table 2. Data may be analyzed down to lower temperatures using an appropriate high-temperature series expansion (HTE).[33−38] The results of least-squares fitting of HTE expressions up to seventh order in J/k_BT are reproduced in Table 2. Values for the

(33) Rushbrooke, G. S.; Wood, P. J. *Proc. R. Soc. London* **1956**, *68*, 1161.
(34) Rushbrooke, G. S.; Wood, P. J. *Mol. Phys.* **1958**, *1*, 257.
(35) Stephenson, P. L.; Pirnie, K.; Wood, P. J.; Eve, J. *Phys. Lett.* **1968**, *25A*, 2.
(36) Yamaji, K.; Kondo, J. *J. Phys. Soc. Jpn.* **1973**, *35*, 25.
(37) Rushbrooke, G. S., Baker, G. A., Wood, P. J. In *Phase transitions and critical phenomena: series expansions for lattice models*; Domb, C., Green, M. S., Eds.; Academic Press: New York, 1974; Vol. III.
(38) Navarro, R. In *Magnetic properties of layered transition metal compounds*; de Jongh, L. J., Ed.; Kluwer: Dordrecht, The Netherlands, 1990.

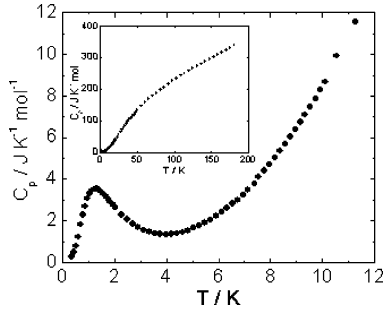

Figure 6. Heat capacity of **1** at low temperature, with data for the full temperature range shown as an inset. The peak around 3 K is believed to arise from 2D magnetic correlations.

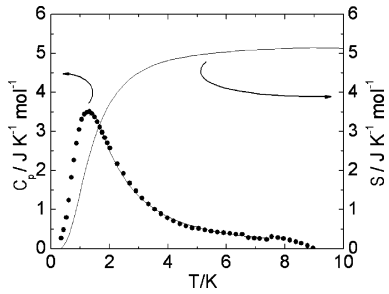

Figure 7. Magnetic contribution to the heat capacity of **1** (solid circles), with the corresponding entropy (solid line). A fit to a HTE expression for the heat capacity is also displayed as a solid line.

moments on Cu^{2+} and Mn^{2+} are reasonably close to the spin-only values, while that for the Co compound is significantly higher, as expected for an ion that will have significant contributions to the moment due to the mixing in of low-lying excited states. The influence of quantum fluctuations on the susceptibility of the $S = {}^1/_2$ system, **1**, is not expected to be significant, at least for the range and resolution in temperature of our measurements.[3,21,37−4139−41]

A key motivation for work on the magnetic properties of compounds such as **1** is to find better examples of 2D QHASLs. To assess its suitability in this respect, we also need values for the interplane exchange, J'. The most direct method to determine J' would be to measure inter- and intraplanar spin-wave dispersion by inelastic neutron scattering, but this requires perdeuterated single crystals on the order of 100 mm^3 in size. Given the present form of the sample, it is more appropriate to measure the magnetic susceptibility or the heat capacity to low temperatures to determine the Néel temperature and from that to estimate an approximate value for J'. No features were observed in the magnetic susceptibility that were indicative of long-range magnetic order down to the lowest temperature that was accessible for us (1.8 K).

Heat Capacity. We were able to access lower temperatures in the determination of C_p, but upon cooling to 0.33 K, we only saw a single, relatively broad maximum centered at 1.3 K and we believe that this is most likely to arise from the buildup of 2D correlations upon cooling (Figure 6). Any 3D transition is expected to be manifested by a sharper feature at lower temperatures; however, as the ratio J'/J falls, this transition becomes less distinct, and for values on the order of 10^{-2} or less, it would be challenging to observe it experimentally.[42] There is therefore indirect evidence that J'/J is relatively small in **1**. Recent quantum Monte Carlo calculations on anisotropic cubic lattices in which exchange is weaker along one axis (J') than within perpendicular, square layers (J) have produced an expirical relation between these parameters and T_N.[43] In the case of $S = {}^1/_2$ for $0.001 < J/J' < 1$, the relationship is

$$T_N = 2.30J/[2.43 - \ln(J'/J)] \quad (2)$$

Thus, for J'/J of the order of 10^{-4} and $J/k_B = 2.1$ K, T_N will be approximately 0.4 K. It is unlikely that J'/J is as small as 10^{-4} in **1**, suggesting that our heat capacity measurements have missed any long-range ordering transition.

We did not have a diamagnetic analogue available at the time of the heat capacity measurements, so we need to consider both phonon and magnetic contributions to C_p for this sample. To isolate the magnetic contribution, we applied a relatively simple correction, fitting data over a region where we believed much of the magnetic entropy had been given up, while still lying well below a likely Debye temperature: data were fitted to the function aT^3, the leading term in the standard expression for the phonon contribution at low temperature,[44] and then extrapolated to $T = 0$. This term was then subtracted from C_p from the lowest experimental temperature of 0.33 K to 10 K to leave what was taken to be the magnetic contribution. This is illustrated in Figure 7, together with the change in the magnetic entropy, ΔS, upon warming from T_1 to T_2, calculated using the expression

$$\Delta S = \int_{T_1}^{T_2} \frac{C_p}{T}\, dT \quad (3)$$

Quantum Monte Carlo calculations[40−42,45] predict a peak in the heat capacity for the 2D $S = {}^1/_2$ Heisenberg antiferromagnet at a temperature of approximately 0.7 J/k_B (i.e., at about 1.5 K), with a value of about 0.4R (i.e., approximately 3.5 J K^{-1} mol^{-1}); our C_p data yield values of 1.28(1) K and 3.49(1) J K^{-1} mol^{-1} for these two quantities, respectively. We also present a fit to the heat capacity data of an appropriate high-temperature expansion up to six terms in J/k_BT over the temperature range 1.5−7.5 K. This yielded the optimized value of $J/k_B = 1.22$ K.[36,38,46] The limiting value of the magnetic entropy should correspond to R ln 2 for a $S = {}^1/_2$ system, equal to 5.762 J K^{-1} mol^{-1}; we find a value of 5.15 J K^{-1} mol^{-1}. The reason for this discrepancy could be overcompensation for the phonon contribution to the heat capacity, and perhaps also the presence of continuing

(39) Takahashi, M. *Phys. Rev. B* **1989**, *40*, 2494.
(40) Makivic, M. S.; Ding, H.-Q. *Phys. Rev. B* **1991**, *43*, 3562.
(41) Kim, J.-K.; Troyer, M. *Phys. Rev. Lett.* **1998**, *80*, 2705.
(42) Sengupta, P.; Sandvik, A. W.; Singh, R. R. P. *Phys. Rev. B* **2003**, *68*, 094423.
(43) Yasuda, C.; Todo, S.; Hukushima, K.; Alet, F.; Keller, M.; Troyer, M.; Takayama, H. *Phys. Rev. Lett.* **2005**, *94*, 217201.
(44) Kittel, C. *Introduction to Solid State Physics*, 6th ed.; Wiley & Sons: New York, 1988; Vol. 1.
(45) Gomez-Santos, G.; Joannopoulos, J. D.; Negele, J. W. *Phys. Rev. B* **1989**, *39*, 4435.
(46) Baker, G. A.; Gilbert, H. E.; Eve, J.; Rushbrooke, G. S. *Phys. Lett.* **1967**, *25A*, 207.

spin disorder and fluctuations (perhaps arising through quantum fluctuations), at low temperatures.

Conclusions

[BDTA]$_2$[MCl$_4$] [M = Cu (**1**), Co (**2**), and Mn (**3**)] was synthesized by a slow diffusion of the appropriate precursor salts in solution. Crystal structures were obtained for **1**−**3** and display a molecular structure of sandwich layers of $[MCl_4]^{2-}$ between two $[BDTA]^+$ layers. In each case, the magnetic coupling is predominantly antiferromagnetic and weak, with the coupling strength increasing as the metal gets heavier: series expansion analysis of the susceptibility data indicates that $J/k_B = 0.018(1)$, 0.35(3), and 2.10(2) K as M runs from Mn to Co to Cu. There is no evidence for magnetic long-range order down to 1.8 K for **2** and **3**, while the heat capacity data for **1** suggest a small ratio J'/J. This last material is, therefore, very promising as a model 2D SQHASL, with small J, and likely to be more amenable to strong tuning by an applied magnetic field than other materials of this class studied to date; we anticipate $H_c \cong 6.3$ T ($H^* \cong 4.6$ T). We have recently prepared small quantities of the Zn analogue of these materials, and although we have not yet obtained samples suitable for single-crystal X-ray diffraction, analysis of powder diffraction data suggests it to be isomorphous with **2** and **3**.[47] This presents a rare opportunity to investigate the influence of doping of the $S = {}^1/_2$ system diamagnetically and testing of the suggestion that this might also enhance nonclassical magnetic effects.[48−52] The next stage of characterization should include the determination of a long-range magnetic ordering temperature for **1**, and the most straightforward way of doing this is probably through muon spin rotation or relaxation measurements,[53−55] before embarking on neutron studies of the response of this material to an applied magnetic field, and a search for novel, quantum disordered phases.

Acknowledgment. We are grateful to The University of Edinburgh, the EPSRC, and the U.K. Joint Infrastructure Fund for financial support and to Professor Kunio Awaga of Nagoya University for the generous supply of [BDTA]-Cl.

Supporting Information Available: X-ray crystallographic data in CIF format. This material is available free of charge via the Internet at http://pubs.acs.org.

IC052024I

(47) de Vries, M. J.; Staniland, S. S. Personal communication, 2005.

(48) Clarke, S. J.; Harrison, A. *J. Phys.: Condens. Matter* **1992**, *4*, 6217.
(49) Clarke, S. J.; Harrison, A. *J. Magn. Magn. Mater.* **1995**, *140*, 1627.
(50) Chernyshev, A. L.; Chen, Y. C.; Neto, A. H. C. *Phys. Rev. B* **2002**, *65*, art. no. 104407.
(51) Vajk, O. P.; Mang, P. K.; Greven, M.; Gehring, P. M.; Lynn, J. W. *Science* **2002**, *295*, 1691.
(52) Sandvik, A. S. *Phys. Rev. B* **2002**, *66*, 024418.
(53) de Reotier, P. D.; Yaouanc, A. *J. Phys.: Condens. Matter* **1997**, *9*, 9113.
(54) Blundell, S. J.; Pratt, F. L.; Lancaster, T.; Marshall, I. M.; Steer, C. A.; Heath, S.; Letard, J. F.; Sugano, T.; Mihailovic, D.; Omerzu, A. *Polyhedron* **2003**, *22*, 1973.
(55) Lancaster, T.; Blundell, S. J.; Pratt, F. L.; Brooks, M. L.; Manson, J. L.; Brechin, E. K.; Cadiou, C.; Low, D.; McInnes, E. J. L.; Winpenny, R. E. P. *J. Phys.: Condens. Matter* **2004**, *16*, S4563.